International Journal of Science and Research (IJSR)
ISSN: 2319-7064
ResearchGate Impact Factor (2018): 0.28 | SJIF (2018): 7.426

Sparse Representation of Image with Immune Clone Algorithm based on Harmonic Wavelet Packet Dictionary

WANG Li, WANG Wei, LIU Boni

[1] Xi'an Aeronautical University, Department of Electronic Engineering, Xi'an Shaanxi 710077, China

Abstract: ***Sparse representation of image could reduce the amount of original data and facilitate the subsequent processing. When using the redundant dictionary to represent the images, we need to look for an efficient optimal algorithm to seek the optimal atoms. In this paper, an immune clone algorithm for sparse representation of image based on harmonic wavelet packet dictionary is proposed. The proposed algorithm relies on the global optimal search ability of immune clone algorithm to realize the process of looking for optimal atoms. The fitness function for immune clone algorithm is designed and the implementation process for sparse representation is shown. Experimental results show that compared with orthogonal matching pursuit algorithm, the proposed algorithm could improve the computational efficiency while guarantee the reconstruction accuracy.***

Keywords: Sparse representation; Harmonic wavelet packet dictionary; Immune clone algorithm; Reconstruction accuracy

1. Introduction

Effective sparse representation could capture the main features of the signal, which leads to achieve a small amount of data for signal description. Its applications include image classification **Error! Reference source not found.**, signal de-noising **Error! Reference source not found.**, object detection [3], and face recognition [4]. Especially in the field of compressed sensing, sparse representation of the signal [5] [6] is the prerequisite for efficient observation. The basic idea of sparse representation is, from the set of basic functions of the signal projection, extracting only a small number of the basic functions could represent the original signal without little distortion. Sparse representation model requires that in the signal expansion, the coefficients of most of the basic functions are zero, only a few basic functions have large non-zero coefficients. The basic function is referred as an atom, and the set of all atoms is called dictionary.

The image is a two-dimensional complex signals with a variety of structural components. It is difficult to form an effective representation with the orthogonal decomposition method, such as the Fourier transform or cosine transform. Increasing the number of atoms in the dictionary to form non-orthogonal dictionary would improve the matching flexibility, which is beneficial for sparse representation of image. When the number of atoms in the dictionary is greater than the signal dimension, the dictionary is over-complete or redundant [7] [8]. Because of the various choice of the redundant dictionary, to design an efficient dictionary is the first event for sparse representation. Meanwhile, since the sparse representation of a signal under such redundant dictionary is not unique, looking for the best combination from all the atoms is the focus.

Many redundant dictionaries have been proposed, such as the wavelet packet dictionary [9] and isotropic Gabor dictionary [10]. The wavelet packet dictionary contains wavelet atoms, but it could not represent the edge structure of image due to its separability and isotropic. Isotropic Gabor dictionary with a single spatial frequency bandwidth Gabor atom is not conducive to capture the geometric structure of the image edge contour regularity. Harmonic wavelet proposed by D. E. Newland has caused attentions. Compared with other wavelet function, harmonic wavelet dictionary [11] [12] has the orthogonality with more general sense and excellent time-frequency decomposition.

The typical way to obtain such signal sparse representation is orthogonal matching pursuit (OMP) algorithm [13]. OMP, an iterative greedy algorithm, chooses the best atom from the dictionary to match the signal which leads high reconstruction accuracy. In order to reduce the computational complexity or improve the reconstruction accuracy, there emerges some improved OMP algorithms [14] [15]. In fact, sparse representation process is a searching process for optimal atoms, the evolutionary algorithms [16] [17] could be used to achieve the sparse representation. Immune clone algorithm (ICA) with global optimal search ability [18] obtains wide attention.

On the basis of above analysis, a sparse representation algorithm with immune clone algorithm based on harmonic wavelet packet dictionary is proposed. The harmonic wavelet packet dictionary is constructed for image sparse representation. The affinity function and the main operators in ICA, including cloning, cloning mutation and cloning selection, are designed. Moreover, the implementation process for searching optimal atoms using ICA is shown. Four classic images are used to test the effectiveness of the proposed algorithm.

The remainder of this paper is arranged as follows. In Section 2, the construction of harmonic wavelet packet redundancy dictionary and the searching process using OMP are introduced. And then in Section 3, the three aspects of the proposed algorithm, namely initial antibody production, affinity function design and main operators design are

presented. Next in Section 4, experimental results are shown and analyzed. Finally, in Section 5, some concluding remarks are made.

2. Dictionary construction and OMP algorithm for sparse representation

The signal sparse representation model based on redundant dictionary is expressed as:

$$\min\|\boldsymbol{\theta}\|_0 \quad s.t. \quad \boldsymbol{x}=\boldsymbol{\Phi}\boldsymbol{\theta} \tag{1}$$

where, $\boldsymbol{x}\in R^N$ is the original signal, $\boldsymbol{\Phi}\in R^{N\times L}$ is the redundant dictionary, and $\boldsymbol{\theta}\in R^L$ is the sparse coefficient vector. Each column in $\boldsymbol{\Phi}$ is called as an atom. In sparse representation, there are two issues needed to be solved: 1) construct the redundant dictionary $\boldsymbol{\Phi}$, and 2) solve the optimal function in equation (1) to obtain the sparse coefficient vector $\boldsymbol{\theta}$. In the following, we first introduce the construction of harmonic wavelet packet redundancy dictionary, and then show the standard sparse representation process using OMP algorithm.

2.1 Construction of harmonic wavelet packet redundancy dictionary

Harmonic wavelet has the following advantages: 1) exact box function form of the spectrum; 2) simple and clear function expression; 3) significant feature of orthogonality and symmetry; 4) simple algorithm implementation. The frequency-domain form of harmonic wavelet with frequency ω is,

$$W_{p,q}(\omega)=\begin{cases}\dfrac{1}{(q-p)2\pi} & 2\pi p\le\omega\le 2\pi q\\ 0 & else\end{cases} \tag{2}$$

where, p and q are the scale parameters, which determine the bandwidth of harmonic wavelet.

The time-domain form of harmonic wavelet is obtained by inverse Fourier transform on Equation (2), n is the time-domain variable,

$$w_{p,q}(n)=\frac{e^{jq2\pi n}-e^{jp2\pi n}}{j2\pi(q-p)n} \tag{3}$$

Given the shift step $v/(q-p)$, v is the translation parameter, do translation transformation, the Equation (3) becomes,

$$w_{p,q,v}(n)=\frac{e^{jq2\pi\left(n-\frac{v}{q-p}\right)}-e^{jp2\pi\left(n-\frac{v}{q-p}\right)}}{j2\pi(q-p)\left(n-\frac{v}{q-p}\right)} \tag{4}$$

To do Fourier transform on Equation (4), the frequency-domain expression is,

$$W_{p,q,v}(\omega)=\begin{cases}\dfrac{1}{(q-p)2\pi}\exp\left(\dfrac{-j\omega v}{q-p}\right) & 2\pi p\le\omega\le 2\pi q\\ 0 & else\end{cases} \tag{5}$$

This is the expression of the generalized harmonic wavelet with bandwidth $(q-p)2\pi$, centered at $v/(q-p)$. Similar to other wavelet decomposition, the analysis frequency domain of the wavelet decomposition becomes small with the number of layers increasing. And the refining capacity in the low-band frequency domain is better than in the high-band frequency domain. For this defect, in order to improve the resolution in the high-band frequency domain, the following method is employed.

Given the harmonic wavelet packet decomposition level s, the corresponding signal would be decomposed into 2^s frequency sub-bands. The highest frequency of the signal decomposition is f_h, thus, the analysis bandwidth of the sub-band of harmonic wavelet packet is,

$$f_{band}=f_h/2^s \tag{6}$$

Because the bandwidth of harmonic wavelet is $(q-p)2\pi$, the scale parameters p and q should satisfy,

$$2\pi(q-p)=2\pi f_{band} \tag{7}$$

Thus, the parameters of harmonic wavelet packet (s,u,v) could establish a close link to the parameters of harmonic wavelet (p,q,v). When the signal dimensional is N, the range of level s is $s=0,1,...,\log_2(N)-1$. The parameter u is the sub-band index, $u=0,1,...,2^s-1$. The third parameter v is the wavelet coefficients index in the sub-band, $v=0,1,...,N-1$. Then the parameters p and q are determined as,

$$p=uf_{band} \tag{8}$$

$$q=(u+1)f_{band} \tag{9}$$

Through this way, at any decomposition level, same high-resolution analysis of the entire frequency domain could be achieved. Given (s,u,v), a harmonic wavelet packet dictionary can be obtained. The number of atoms in a harmonic wavelet packet dictionary is $N(N-1)$.

2.2 OMP algorithm for sparse representation

As the l_0 norm is non-convex, solving signal sparse representation under a redundant dictionary is a NP-hard problem. There does not exist known polynomial time algorithm to solve this optimization problem, a sub-optimal approximation method is needed. The OMP is a greedy algorithm to obtain the sparse representation of signal. The implementation process of OMP is summarized as follows:

1) Initialize the iterative number $k=1$, residual $\boldsymbol{r}_0=\boldsymbol{x}$, index collection of optimal atoms $\Lambda_0=[]$.
2) Traversal all the atoms in matrix $\boldsymbol{\Phi}$ to select the index of optimal matching atom, $\lambda_k=\arg\max_l\left|\langle\boldsymbol{r}_{k-1},\boldsymbol{\Phi}_l\rangle\right|$, wherein $\boldsymbol{\Phi}_l$ is l-th column of $\boldsymbol{\Phi}$.
3) Update index collection, $\Lambda_k=\Lambda_{k-1}\bigcup\lambda_k$.
4) Update residual, $\boldsymbol{r}_k=\boldsymbol{x}-\boldsymbol{\Phi}_{\Lambda_k}\left(\boldsymbol{\Phi}_{\Lambda_k}^{\mathrm{T}}\boldsymbol{\Phi}_{\Lambda_k}\right)^{-1}\boldsymbol{\Phi}_{\Lambda_k}^{\mathrm{T}}\boldsymbol{x}$, wherein $\boldsymbol{\Phi}_{\Lambda_k}$ represents the sub-matrix constructed by the atoms indexed by Λ_k.
5) Determine whether the maximum iteration number K is satisfied, if not then $k=k+1$, repeat 2)~4), else stop iteration.

In other words, the maximum iteration number in OMP is the number of optimal atoms to represent the original signal. The original signal $\boldsymbol{x}$ could be represented using the K optimal atoms indexed by Λ_K. The sparse coefficient vector is,

$$\hat{\theta} = \left(\boldsymbol{\Phi}_{\Lambda_K}^{\mathrm{T}} \boldsymbol{\Phi}_{\Lambda_K}\right)^{-1} \boldsymbol{\Phi}_{\Lambda_K}^{\mathrm{T}} \boldsymbol{x} \tag{10}$$

where $\boldsymbol{\Phi}_{\Lambda_K}$ represents the sub-matrix consisting of column vectors in $\boldsymbol{\Phi}$ indexed by Λ_K.

After getting the sparse representation form of the signal, we need to reconstruct the signal using the dictionary and the sparse coefficient vector. The reconstructed signal is expressed as,

$$\hat{\boldsymbol{x}} = \boldsymbol{\Phi}_{\Lambda_K} \hat{\boldsymbol{\theta}} \tag{11}$$

3. Proposed algorithm using ICA for sparse representation

Seen from the above process of OMP, the algorithm needs to traversal every atom in the redundant dictionary. If the dictionary has a higher redundancy, the computational complexity of OMP would be unbearable. In this paper, the evolutional algorithm ICA is explored to achieve the searching process of optimal atoms. The organizing construction of this section is as follows. First of all, the framework of the proposed algorithm is shown. And then, the three major aspects in the proposed algorithm, including the initial antibody production, the affinity function design and the main operators, are presented. Finally, the implementation process is summarized.

3.1 Framework of proposed algorithm

Instead of traversal every atom as OMP, ICA commits to imitate the natural immune system, with learning and memory function, which provides a new method for information processing. As a global optimization search algorithm, ICA takes into account the ability of global and local search, with taking the advantages of parallel search of genetic algorithm. Meanwhile, ICA introduces the affinity of mature, cloning and memory mechanisms, and utilizes the appropriate operators to ensure that the algorithm could quickly converge to the global optimal solution. Instead of the greedy pursuit method, ICA is applied to search the optimal atoms for image sparse representation.

It should be declared that once the original signal is determined, the redundant dictionary could be constructed using the way introduced in section 2.1. The goal of the proposed algorithm is to seek the best optimal atoms to represent the original signal, thereby obtaining the reconstructed signal. The framework of the proposed algorithm is shown in Figure 1. In ICA, antibody is the candidate solution for the object optimal problem, and antigen represents the object optimal problem. Referred to our optimal problem, the antigen is the optimal problem expressed in equation (1) and one antibody represents a combination of the atoms selected from the redundant dictionary. Seen from the figure, the first thing in the proposed algorithm is to produce the initial antibody in the population. Then the affinity function, used for calculating the affinity between the antibody and antigen, needs to be designed. The core in the algorithm is designing the three operators, including cloning, cloning mutation and cloning selection, to search for the best antibody. Through continuous evolution process, the best antibody is generated and the sparse coefficient could be achieved.

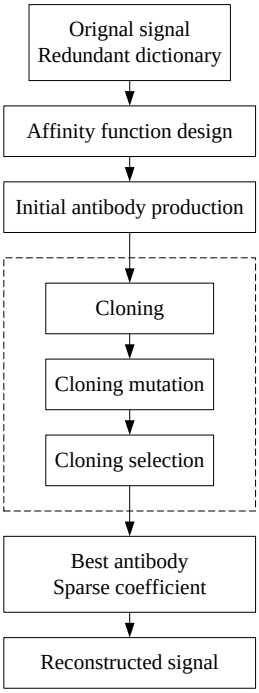

Figure 1: The framework of the proposed algorithm

3.2 Specific details of proposed algorithm

In this subsection, the specific details in the proposed algorithm are presented. We would give the initial antibody production process, and the designed affinity function. Then we would present how to obtain the best antibody through the three operators.

3.2.1 Initial antibody production

Assume the number of optimal atoms is K, then the antibody is expressed as a $1 \times K$ row vector, such as $a = \left(aa^1, aa^2, ..., aa^K\right)$, where aa^k is one number of set $[1, L]$, represents one atom in the dictionary. A population contains a number of antibodies, that is $A = \left(a_1; a_2; ...; a_Q\right)$, where Q is the population size.

3.2.2 Affinity function design

In ICA, affinity function indicates the objective function value of candidate solution, and is used to evaluate the pros and cons of the antibodies, finally to guide the cloning operator. The antibody is more excellent with higher affinity. In order to find the optimal atoms to describe one image under redundant dictionary, the affinity function is designed as follows,

$$affinity(a) = 1 \Big/ \left\| \boldsymbol{x} - \boldsymbol{\Phi}_a \boldsymbol{\theta}_a \right\|_2^2 \tag{12}$$

where, $\boldsymbol{\Phi}_a$ and $\boldsymbol{\theta}_a$ are the corresponding atoms and coefficients selected by antibody a.

3.2.3 Three operators design

(1) Cloning operator

Cloning operator done on the population A,

$$\vartheta(A)=\left(\vartheta(a_1);\vartheta(a_2);...;\vartheta(a_Q)\right) \quad (13)$$

where, $\vartheta(a_i)$ is the clone of a_i. The clone number is defined as,

$$C_i = C\frac{affinity(a_i)}{\sum_{q=1}^{Q} affinity(a_q)} \quad (14)$$

where, C is the clone consistent.

After cloning operator, the population turns to,

$$A=\left(A;A_1';A_2';...;A_Q'\right) \quad (15)$$

where, $A_i'=\left(a_{i1};a_{i2};...;a_{iC_i-1}\right)$, $a_{iq}=a_i$, $q=1,2,...,C_i-1$.

(2) Cloning mutation operator

In order to retain the original information of the antibody, the mutation operator is only applied to clone antibodies $\vartheta(a_i)$. Specify mutation probability P_{m}, for each component of the antibody, generates a random number pm between 0 and 1. If $pm<P_{\mathrm{m}}$, then the corresponding component would be re-selected as one number from set $[1,L]$, otherwise the component would not change.

(3) Cloning selection operator

If there exists the outstanding mutation antibody $b=\max\left\{affinity(a_{iq})\middle|q=1,2,...,C_i-1\right\}$ which satisfies,

$$affinity(a_i)<affinity(b) \quad a_i\in A \quad (16)$$

then antibody b is chosen to replace the parent antibody a_i to update the population.

After the three operators, the initial population would be evolved to the next generation population which has higher affinity. The best antibody a_{best} is obtained by implementing the above process in an iterative fashion. Then the sparse coefficient would be expressed as,

$$\hat{\boldsymbol{\theta}}=\left(\boldsymbol{\Phi}_{a_{best}}^{\mathrm{T}}\boldsymbol{\Phi}_{a_{best}}\right)^{-1}\boldsymbol{\Phi}_{a_{best}}^{\mathrm{T}}\boldsymbol{x} \quad (17)$$

where $\boldsymbol{\Phi}_{a_{best}}$ is the corresponding atoms selected by the best antibody a_{best}.

3.3 Implementation process of the proposed algorithm

Based on the value of the affinity function, continuously updating the scale of the population by cloning through an iterative way, the proposed algorithm tries to find the optimal atoms to describe the image. Then the sparse coefficients could be calculated and finally the original image would be represented sparsely. The block diagram of the proposed algorithm is depicted in Figure 2, and the implementation process is summarized as follows.

1) Initialization: set evolution generation $m=1$, set the initial antibody population $A^1=\left(a_1;a_2;...;a_Q\right)$.
2) Affinity computing: Compute the affinity of each antibody in A^m using equation (12).
3) Cloning operating: Calculate clone number of each antibody according to equation (14), achieve the clone population using equation (15).
4) Cloning mutation operating: Generates a random number pm to determine whether the component of antibody would change.
5) Cloning selection operating: Update the population according to equation (16), obtain the population A^{m+1}.
6) Stopping criterion: Determine whether the maximum evolution generation M is satisfied, if not then $m=m+1$, repeat (2)~(5), else stop iteration.
7) Best antibody: Compute the affinity of each antibody in A^M, choose the best antibody a_{best} with the highest affinity.
8) Sparse coefficient computing: Compute the sparse coefficient using equation (17).

The reconstructed signal could be expressed as,

$$\hat{\boldsymbol{x}}=\boldsymbol{\Phi}_{a_{best}}\hat{\boldsymbol{\theta}} \quad (18)$$

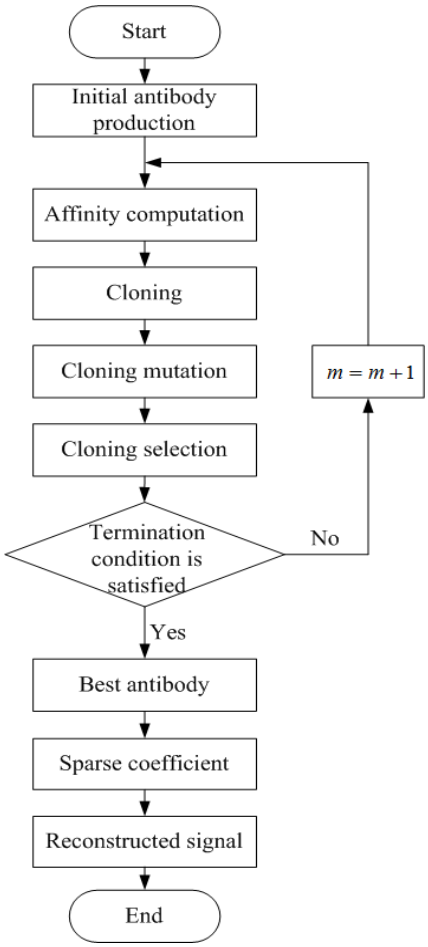

Figure 2: Block diagram of proposed algorithm

4. Experimental Results and Analysis

In order to evaluate the performance of the proposed algorithm, some experimental results and analysis on four classic images are carried out in this section. At the beginning, the parameter for OMP algorithm is determined. Next, the parameters for proposed algorithm ICA are determined. And

then, the comparison between the proposed algorithm ICA and standard OMP algorithm is shown, using peak signal-to-noise ratio (PSNR), structural similarity (SSIM) [19] and runtime to assess the performance. The hardware and software environments for these experiments are: AMD quad-core CPU, 3.80GHz, 16G memory and Matlab2012b.

The four images shown in Figure 3 are Cameraman, Barbara, Lena and Peppers with spatial size 256×256. Seen from the implementation processes of OMP and the proposed algorithm, the computational complexity has positive correlation with the dictionary dimension L. If the global image is processing as the original signal, the dimension N would be 65536. Then the dictionary dimension L would reach four billion, leading the computing time unable to estimate. Therefore, in the following experiments, the images are divided into blocks to process. The block size is set as 8 without losing generality. In other words, the dimension of signal processed in the algorithms is 64 and the dictionary contains 4032 atoms.

Figure 3: Four test images. (a) Cameraman, (b) Barbara, (c) Lena and (d) Peppers.

Two metrics are adopted to evaluate the reconstruction accuracy of the proposed algorithm, PSNR and SSIM between the reconstructed image and the original image. The PSNR measured in dB is defined as,

$$\mathrm{PSNR}(\boldsymbol{x},\hat{\boldsymbol{x}}) = 20\log_{10}\frac{\max(\boldsymbol{x})}{\sqrt{\mathrm{MSE}(\boldsymbol{x},\hat{\boldsymbol{x}})}} \tag{19}$$

where $\boldsymbol{x}$ and $\hat{\boldsymbol{x}}$ are the original and reconstructed image, $\max(\boldsymbol{x})$ is the peak value of $\boldsymbol{x}$, $\mathrm{MSE}(\boldsymbol{x},\hat{\boldsymbol{x}})$ is the mean squared error,

$$\mathrm{MSE}(\boldsymbol{x},\hat{\boldsymbol{x}}) = \frac{1}{N}\|\boldsymbol{x}-\hat{\boldsymbol{x}}\|_2^2 \tag{20}$$

The SSIM between $\boldsymbol{x}$ and $\hat{\boldsymbol{x}}$ is defined as,

$$\mathrm{SSIM}(\boldsymbol{x},\hat{\boldsymbol{x}}) = \frac{(2\mu_1\mu_2+C_1)(2\sigma_{12}+C_2)}{(\mu_1^2+\mu_2^2+C_1)(\sigma_1^2+\sigma_2^2+C_2)} \tag{21}$$

where μ_1 and μ_2 are the mean values of $\boldsymbol{x}$ and $\hat{\boldsymbol{x}}$, σ_1 and σ_2 are the standard deviation values of $\boldsymbol{x}$ and $\hat{\boldsymbol{x}}$, σ_{12} represents the correlation coefficient between $\boldsymbol{x}$ and $\hat{\boldsymbol{x}}$, C_1 and C_2 are constants related to the dynamic range of the pixel values. The details for these parameters can refer to [20].

4.1 Parameter selection for OMP

There is no doubt that the parameter selection would have significant effect on performance. In the implementation process of OMP, the maximum iteration number K, i.e., the number of optimal atoms, should be determined firstly. In this part, experiments on four images using OMP with different K are presented. The atom number is varied from 1 to 100 at the interval of 1. The reconstructed images are represented by the optimal K atoms. The PSNR and SSIM of Cameraman and Lena are shown in Figure 4 and Figure 5, respectively.

It is not surprising that, with the increase of the atom number, the reconstructed PSNR is increasing as well. The weird thing is that when the atom number reaches about 35, the PSNR has a sharp jump. The reason for this phenomenon is not known, but it is certain that these atoms are very important for the representation of the image. Meanwhile, we noticed that the PSNR is not keeping improve with the atom number. When the atom number increases to 40, PSNR would tend to be smooth. That is to say, the sparsity level of images under this harmonic wavelet packet dictionary is 40. The SSIM is also increasing with the atom number K, and it tends to be stable after K reaches 40. The results of other two images are similar with these two images. Therefore, in the following experiments, the atom number in OMP is selected as 40.

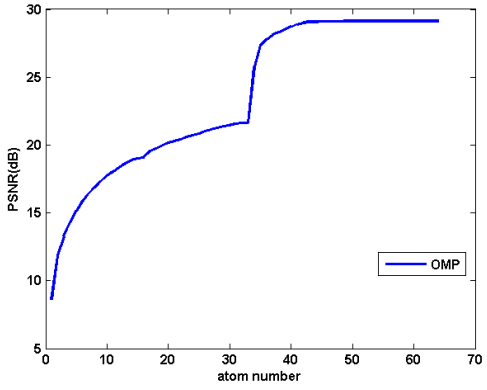

(a) PSNR

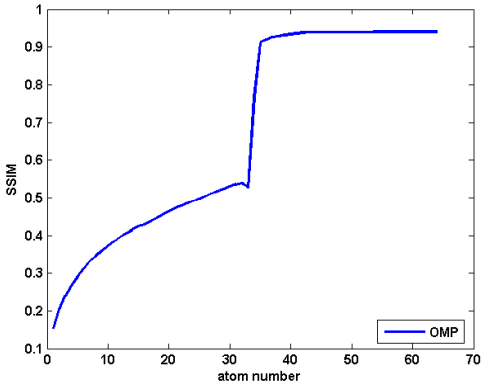

(b) SSIM

Figure 4: The PSNR and SSIM of Cameraman with different maximum iteration number.

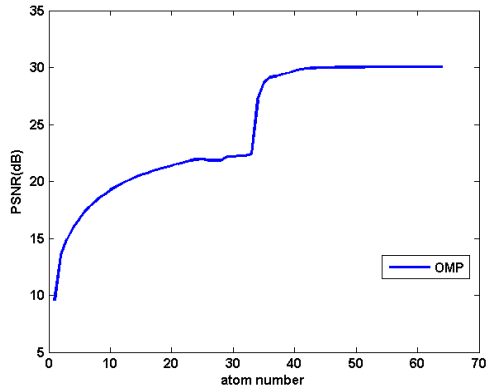

(a) PSNR

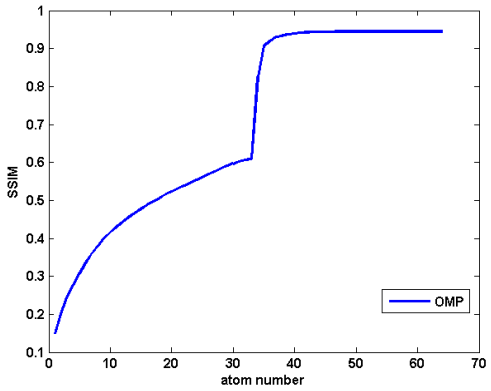

(b) SSIM

Figure 5: The PSNR and SSIM of Lena with different maximum iteration number

4.2 Parameter selection for proposed algorithm

In the implementation process of proposed algorithm, the maximum evolution generation M, the population size Q and the optimal atom number K would have significant effect on the performance of ICA. In this part, experiments on four images using ICA with different parameters are presented. The maximum evolution generation M and the population size Q are varied from 1 to 10 at the interval of 1. The optimal atom number K is varied from 8 to 64 at the interval of 8. In addition, the clone consistent C and mutation probability P_m are set as $C=15$ and $P_m=0.2$. The reconstructed images are represented by the optimal K atoms. Since ICA algorithm is randomness, the simulation would run 10 times under the same parameter to obtain the average value. The average PSNR and time of Barbara with different parameters are shown in Figure 6.

When the optimal atom number K is fixed at 40, the PSNR and time change with the maximum evolution generation M and the population size Q is shown in Figure 6(a). Seen from the figure, the variation of PSNR is not significant with the increase of population size or the evolutionary generation. It is not confirmed that which parameter has the more important effect on the reconstruction performance. From the point of time consuming, shown in Figure 6(b), compared with population size, evolutionary generation has greater influence on computational complexity. Therefore, for the choice of evolutionary generation, it is necessary to consider both the reconstruction accuracy and the computational complexity.

When the population size Q is fixed at 10, the PSNR and time change with the maximum evolution generation M and the optimal atom number K is shown in Figure 6(c). With the increase of maximum evolution generation or optimal atom number, the reconstructed PSNR would gradually improve. Compared with the evolution generation, increasing optimal atom number is more conducive to the improving in reconstruction accuracy. Particularly, when the atom number reaches 40, the influence of evolution generation on PSNR is very weak. From the view of computing time (Figure 6(d)), compared with optimal atom number, the evolution generation would increase the computational complexity more. Therefore, when the atom number is selected large enough, the evolution generation can be selected relatively small. This selection could meet the requirements of the reconstruction accuracy, while reducing the computational complexity of the algorithm.

When the maximum evolution generation M is fixed at 1, the PSNR and time change with the population size and the optimal atom number K is shown in Figure 6(e) and Figure 6(f). Seen from the figure, with the increase of population size, the variation of PSNR is very small, which clearly shows that the population size has little effect on the reconstruction accuracy. When the atom number reaches 40, the reconstruction performance tends to be stable. Seen the time variation shown in Figure 6(f), the computation time has little change with the increase of population size. This is sufficed to say that compared with atom number, the effect of population size on computation time could be ignored.

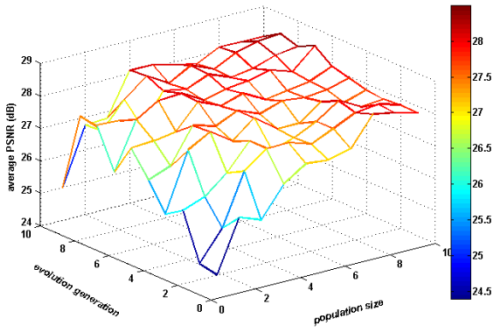

(a) atom number is fixed at 40, the PSNR changes with the evolution generation and the population size.

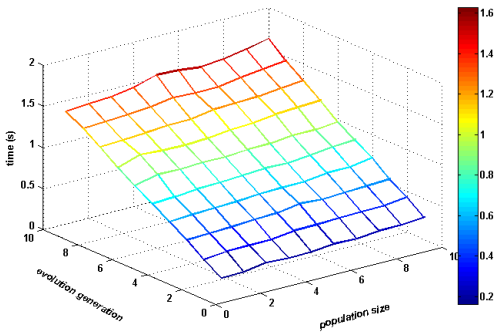

(b) atom number is fixed at 40, the computation time changes with the evolution generation and the population size.

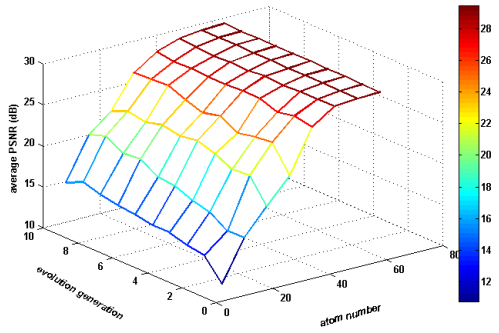

(c) population size is fixed at 10, the PSNR changes with the evolution generation and the atom number.

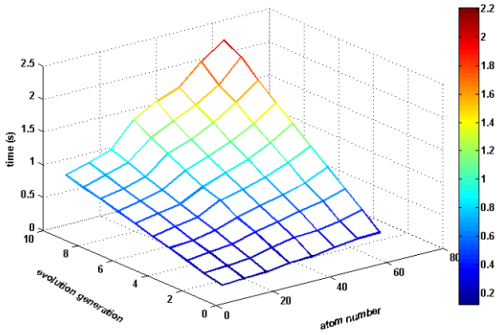

(d) population size is fixed at 10, the computation time changes with the evolution generation and the atom number.

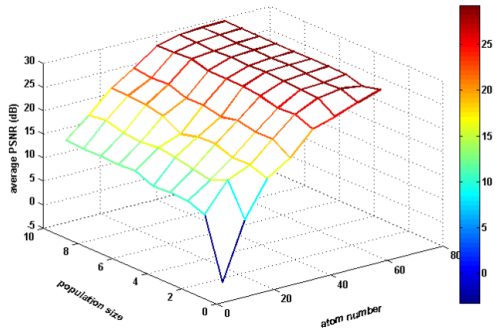

(e) evolution generation is fixed at 1, the PSNR changes with the population size and the atom number.

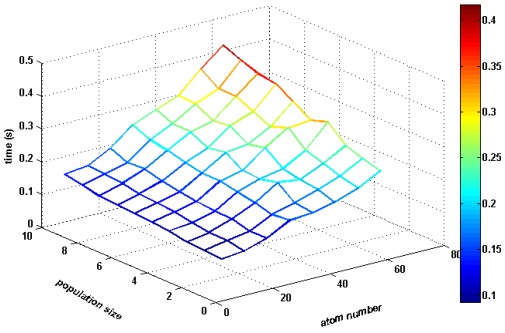

(f) evolution generation is fixed at 1, the computation time changes with the population size and the atom number.

Figure 6: The effects of parameters on reconstructed PSNR and computation time

In summary, from the view of reconstruction quality, seen from the comparison among Figure 6(a), (c) and (e), the atom number has the greatest influence on PSNR. Under the same atom number, PSNR has little change with the increase of population size, while it has weaker increase with evolution generation. From the view of computational complexity, seen from the comparison among Figure 6(b), (d) and (f), evolution generation has the most effect on computation time. Under the same atom number, the computation time is linearly increasing with the increase of evolution generation. Therefore, the atom number in proposed algorithm should be selected large enough, while the other two parameters should be selected relatively small. The results of other three images are similar with the shown results. Considering the reconstruction accuracy and the computational complexity, in the following experiments, the population size is selected as $Q=10$, the maximum evolution generation is set as $M=1$ and the optimal atom number is set as $K=40$.

4.3 Comparison between OMP and proposed algorithm

In this subsection, the comparison between standard OMP algorithm and the proposed ICA algorithm is presented. The four images are sparse represented using the optimal atoms searched by OMP and ICA, respectively. The reconstructed PSNR, SSIM and computation time are used to evaluate the performance of the algorithm. The optimal atom number in OMP is $K=40$. The parameters in ICA are $Q=10$, $M=1$ and $K=40$. Because of the randomness of proposed ICA algorithm, the simulation of proposed ICA algorithm would run 10 times to reduce the randomness. In Table 1, the average PSNR and its standard variation are given. Meanwhile, the average SSIM and its standard variation are also given.

Above all, seen from the table, the PSNR of OMP and ICA are comparable, which fully states that by searching optimal atoms using the biological evolution manner, the proposed ICA could achieve the same reconstruction accuracy as that of OMP. Similarly, the SSIM of two algorithms could both reach 0.9, which demonstrates that the optimal atoms searched by the two algorithms could describe the structure of the images very well. Though the proposed algorithm has randomness, the results demonstrate that the fluctuation of PSNR and SSIM are not very significantly.

Next, the computation efficiency of these two algorithms is analyzed. The computation time in Table 1 is the time consuming on the searching atoms. Since the OMP algorithm needs to traversal all the atoms in the redundant dictionary, the complexity is large. Yet, the proposed algorithm utilizes a completely different searching method. It utilizes one antibody to stand for all the optimal atoms, and the best antibody is obtained through evolution. Compared with OMP, the proposed algorithm could save half the time, and the Acceleration ratio reaches about 2. This fully demonstrates that the proposed algorithm could improve the computation efficiency while ensuring the reconstruction accuracy.

Table 1: The comparison between OMP and proposed algorithm

Algorithm	PSNR/dB	SSIM	Time/s	Acceleration ratio
Cameraman				
OMP	28.7175	0.9342	813.5887	1

ICA	28.6168±0.1982	0.9298±0.0052	412.0589	1.9744
Barbara				
OMP	27.6625	0.9078	812.3266	1
ICA	27.3148±0.2545	0.9006±0.0047	426.3560	1.9053
Lena				
OMP	29.7002	0.9393	832.2483	1
ICA	29.5471±0.1714	0.9347±0.0037	421.9676	1.9723
Peppers				
OMP	28.1052	0.9227	852.8380	1
ICA	28.1025±0.1069	0.9172±0.0050	410.0266	2.0800

The comparison between the reconstructed image and the original image are shown in Figure 7 and Figure 8. Limited to the length of the paper, the results of Lena and Peppers are given here. Utilizing OMP for sparse representation, the reconstructed PSNR could reach 29.7002dB and 29.5790dB, while the reconstructed PSNR of the proposed algorithm could reach 28.1052dB and 28.1294dB. The two algorithms can effectively sparse represent the original images. From the view of subjective visual effect, the two groups of reconstructed images can be a good description of the original images.

Figure 7: The reconstructed images and original image of Lena. (a) Original image, (b) reconstructed image using OMP, and (c) reconstructed image using proposed algorithm.

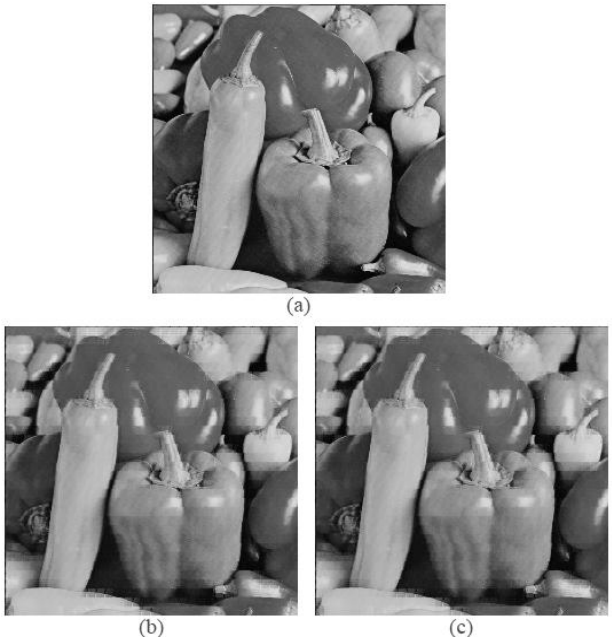

Figure 8: The reconstructed images and original image of Peppers. (a) Original image, (b) reconstructed image using OMP, and (c) reconstructed image using proposed algorithm.

5. Conclusion

In order to obtain sparse representation of image, harmonic wavelet packet dictionary with time-frequency characteristics is constructed in this paper. Aimed at the disadvantage for the high computational complexity of OMP algorithm, the immune clone algorithm for sparse representation of image with lower computational complexity is proposed. Experimental results on four standard test images illustrate that harmonic wavelet packet dictionary could provide sparse representation for the original images. More importantly, the results also demonstrate that compared with OMP algorithm, the proposed ICA algorithm could reduce the computational complexity while ensure reconstruction accuracy. In the future, how to further improve the computation efficiency is the research focus.

6. Acknowledgements

This work was supported by the National Natural Science Foundation of China (grant number 61901350); Scientific Research Plan Projects of Shaanxi Education Department (grant number 19JK0432) and Science Research Fund of Xi'an Aeronautics University (grant number 2019KY0208).

References

[1] CHEN S, ZHOU Y, QI R. Joint sparse representation of hyperspectral image classification based on kernel function [J]. Systems Engineering and Electronics, 2018, 40(3): 692-698. DOI: 10.3969 /j.issn. 1001-506X. 2018. 03. 31.

[2] SONG X, WU L and HAO H. Hyperspectral Image Denoising base on Adaptive Sparse Representation [C]. 2018 IEEE Third International Conference on Data

Science in Cyberspace (DSC), Guangzhou, 2018, pp. 735-739
[3] Yao L. and X. Du. Identification of Underwater Targets Based on Sparse Representation [J]. IEEE Access, 2020, (8): 215-228.
[4] Shoubiao Tan, Xi Sun, Wentao Chan, Lei Qu and Ling Shao. Robust face recognition with kernelized locality-sensitive group sparsity representation [J]. IEEE transactions on image processing, 2017, 26(10), 4661-4668.
[5] K. Guo, X. Xie, X. Xu and X. Xing. Compressing by Learning in a Low-Rank and Sparse Decomposition Form [J]. IEEE Access, vol. 7, pp. 150823-150832, 2019.
[6] R. Zhao, Q. Wang, X. Ma and Z. Qian. Adaptive Sparse Representation for Kronecker Compressive Sensing [C]. 2019 IEEE International Instrumentation and Measurement Technology Conference (I2MTC), Auckland, New Zealand, 2019, pp. 1-6.
[7] A. Seghouane, A. Iqbal and K. Abed-Meraim. A Sequential Block-Structured Dictionary Learning Algorithm for Block Sparse Representations [J]. IEEE Transactions on Computational Imaging, vol. 5, no. 2, pp. 228-239, June 2019.
[8] S. Ayas, E. T. Görmüş and M. Ekinci. A novel pan sharpening method via sparse representation over learned dictionary [C]. 2018 26th Signal Processing and Communications Applications Conference (SIU), Izmir, 2018, pp. 1-4.
[9] Jing Hou, Yuan Wang, Tian Gao, Yan Yang. Fault feature extraction of power electronic circuits based on sparse decomposition [C]. 2016 International Conference on Condition Monitoring and Diagnosis (CMD), 25-28 Sept. 2016, Xi'an, China
[10] Gilles Chardon, Thibaud Necciari, Peter Balazs. Perceptual matching pursuit with Gabor dictionaries and time-frequency masking [C]. 2014 IEEE International Conference on Acoustics, Speech and Signal Processing (ICASSP), 4-9 May 2014, Florence, Italy
[11] Xiaoyun Sun, Zhiyuan Wang, Fengning Kang, Weifang Li. Method of rock bolts parameters detection based on harmonic wavelet packet transform [C]. 2015 International Conference on Machine Learning and Cybernetics (ICMLC), 12-15 July 2015, Guangzhou, China
[12] J. Qiu, J. K. Zao, P. Wang and Y. Chou. Consistent sparse representations of EEG ERP and ICA components based on wavelet and chirplet dictionaries [C]. 2010 Annual International Conference of the IEEE Engineering in Medicine and Biology, Buenos Aires, 2010, pp. 4014-4019.
[13] A. Kulkarni and T. Mohsenin. Low Overhead Architectures for OMP Compressive Sensing Reconstruction Algorithm [C]. IEEE Transactions on Circuits and Systems I: Regular Papers, vol. 64, no. 6, pp. 1468-1480, June 2017.
[14] L. Kang, J. Huang and J. Huang. Adaptive Subspace OMP for Infrared Small Target Image [C]. 2018 14th IEEE International Conference on Signal Processing (ICSP), Beijing, China, 2018, pp. 445-449.
[15] S. Ganguly, I. Ghosh, R. Ranjan, J. Ghosh, P. K. Kumar and M. Mukhopadhyay. Compressive Sensing Based Off-Grid DOA Estimation Using OMP Algorithm [C]. 2019 6th International Conference on Signal Processing and Integrated Networks (SPIN), Noida, India, 2019, pp. 772-775.
[16] S. Shivagunde and M. Biswas, Saliency Guided Image Super-Resolution using PSO and MLP based Interpolation in Wavelet Domain [C]. 2019 International Conference on Communication and Electronics Systems (ICCES), Coimbatore, India, 2019, pp. 613-620.
[17] R. Wang, Y. Wu, M. Shen and W. Cao. Sparse Representation for Color Image Based on Geometric Algebra [C]. 2018 IEEE International Conference on Multimedia and Expo (ICME), San Diego, CA, 2018, pp.1-6.
[18] Khorani. V., Forouzideh. N, and Nasrabadi. A.: Artificial neural network weights optimization using ICA, GA, ICA-GA and R-ICA-GA: Comparing performances [J]. Hybrid Intelligent Models and Applications (HIMA), 2011 IEEE Workshop On. IEEE, 2011, pp. 61-67.
[19] WANG L, FENG Y. Compressed Sensing Reconstruction of Hyperspectral Images Based on Spatial-spectral Multihypothesis Prediction [J]. Journal of Electronics & Information Technology, 2015, 37(12): 3000-3008.
[20] Li Wang, Yan Feng, Yanlong Gao, Zhongliang Wang, Mingyi He. Compressed Sensing Reconstruction of Hyperspectral Images Based on Spectral Unmixing [J]. IEEE Journal of Selected Topics in Applied Earth Observation and Remote Sensing, 2018, 11(4): 1266-1284.

Author Profile

WANG Li received the B.E. degree in electronic and information engineering from Xi'an University of Architecture and Technology, Xi'an, China, in 2009 and the M.S. degree in signal and information processing from Beihang University, Beijing, China, in 2012. She received the Ph.D. degree from Northwestern Polytechnical University, Xi'an, China, in 2018. She now is an lecturer in Xi'an Aeronautics University. Her research interests include compressed sampling, hyperspectral image processing, and optimization algorithm.

WANG Wei received the B.E. degree in electronics and information technology, the Master's degree in aerospace propulsion theory and engineering and the Ph.D. degree in electronic science and technology from the Northwestern Polytechnical University, Xi'an, China. Since 2015, he has been a lecturer in Xi'an Aeronautics University. His current research interests include antenna and radome design, electromagnetic scattering analysis and intelligent optimization algorithm.

LIU Boni received the B.E. degree in Technique of Measuring Control and Instrument from Xi'an Shiyou University, Xi'an, China, in 2003 and the M.S. degree in geodesy and engineering major from Xi`an University of Science and Technology, Xi'an, China, in

2006. Since 2006, she has been an lecturer in Xi'an Aeronautics University. Her research interests include communication technology and electronic measurement.